

## INVESTIGATING THE LOCAL RESERVOIR AGE AND STABLE ISOTOPES OF SHELLS FROM SOUTHEAST ARABIA

Susanne Lindauer<sup>1,2\*</sup> • Soraya Marali<sup>3</sup> • Bernd R Schöne<sup>3</sup> • Hans-Peter Uerpmann<sup>4</sup> • Bernd Kromer<sup>1</sup> • Matthias Hinderer<sup>2</sup>

<sup>1</sup>Curt-Engelhorn-Zentrum Archaeometry gGmbH, Klaus-Tschira-Archaeometry-Centre, C4, 8, 68159 Mannheim, Germany.

<sup>2</sup>Institute of Applied Geosciences, Technical University Darmstadt, Schnittspahnstr. 9, 64287 Darmstadt, Germany.

<sup>3</sup>Institute of Geosciences, University of Mainz, Joh.-J.-Becherweg 21, 55128 Mainz, Germany.

<sup>4</sup>Center for Scientific Archaeology, Eberhard-Karls-University Tübingen, Rümelinstraße 23, 72070 Tübingen, Germany.

**ABSTRACT.** We recently started a systematic approach to determine the reservoir age in southeast Arabia and its dependence on mollusk species and their environment. This part of the study concentrates on local reservoir age and stable isotopes of the lagoonal species *Terebralia palustris* and *Anadara uropigimelana* at Khor Kalba, Oman Sea. Environmental and nutritive influences on mollusks are reflected in the radiocarbon and stable isotope signal. We found a local reservoir age of *A. uropigimelana* of about 940 yr and that of *T. palustris* as 800 yr. Sclerochronological analyses yielded information about seasonality of growth and death in *A. uropigimelana*. The modern shell of *Periglypta reticulata* shares food resources and habitat with *Anadara* sp., of which we did not find a modern specimen. It provided information on response to changes in temperature in the lagoonal system needed for suitability as reflecting climatic conditions. We were interested in carbon pathways of the mangrove in Kalba and a mangrove planted anew on a former mangrove sediment in Ajman. Being an obvious source of charcoal and food of *T. palustris* makes this information necessary. Further analyses will be performed to interpret changes in reservoir age in complex lagoonal systems as reaction to environmental variability.

**KEYWORDS:** <sup>14</sup>C, reservoir effect, mangroves, *T. palustris*, *A. uropigimelana*, *P. reticulata*, stable isotopes, sclerochronology, United Arab Emirates, Oman Sea.

### INTRODUCTION

The coastal areas of southeast Arabia (see map, Figure 1) have been inhabited by humans for thousands of years and represent a possible way “out of Africa” for *Homo sapiens* (Armitage et al. 2011). Due to the arid climate prevailing there since the middle Holocene, establishing accurate chronologies based on radiocarbon dating can be very challenging. Charcoal can sometimes be found as distinct fragments, but often as part of an ashy sediment layer. Organic material like bone collagen, wood, or seeds are often badly preserved if available at all. Inorganic material like bone apatite can easily exchange carbon with its surrounding. Recently, Antoine Zazzo and colleagues (Zazzo et al. 2013; Zazzo 2014) published promising results by using bone apatite. Unfortunately, at our sites no bone material was found in the same context.

The most widespread marine material found at excavations along the coasts are shells, often accumulated to shell middens of up to several meters height. The shells commonly show an older age as indicated by archaeology or <sup>14</sup>C dating from contemporaneous terrestrial organic materials, which is known as the reservoir age, or R(t) (Dutta 2008). In the course of establishing a calibration curve for the ocean environment, several reservoir ages have been determined using specimens from museum collections, collected alive (i.e. during the pre-bomb era). For the Indian Ocean, to which our study area belongs, local reservoir ages for several areas in the Arabian Sea were determined, ranging from 486 yr in Dohar, Qatar, to 501 yr in Muscat, Oman (Southon et al. 2002) in comparison to values of 441 yr in the Arabian Gulf and 583 yr along the Gulf of Oman (Dutta 2008). In Ra’s al-Hamra, Oman, Zazzo and colleagues determined a reservoir age of  $568 \pm 56$  <sup>14</sup>C yr for the 5th millennium BC (Zazzo et al. 2012) and  $645 \pm 40$  yr for the 4th millennium BC (Zazzo et al. 2016). The reservoir age can be variable over

\*Corresponding author. Email: Susanne.lindauer@cez-archaeometrie.de.

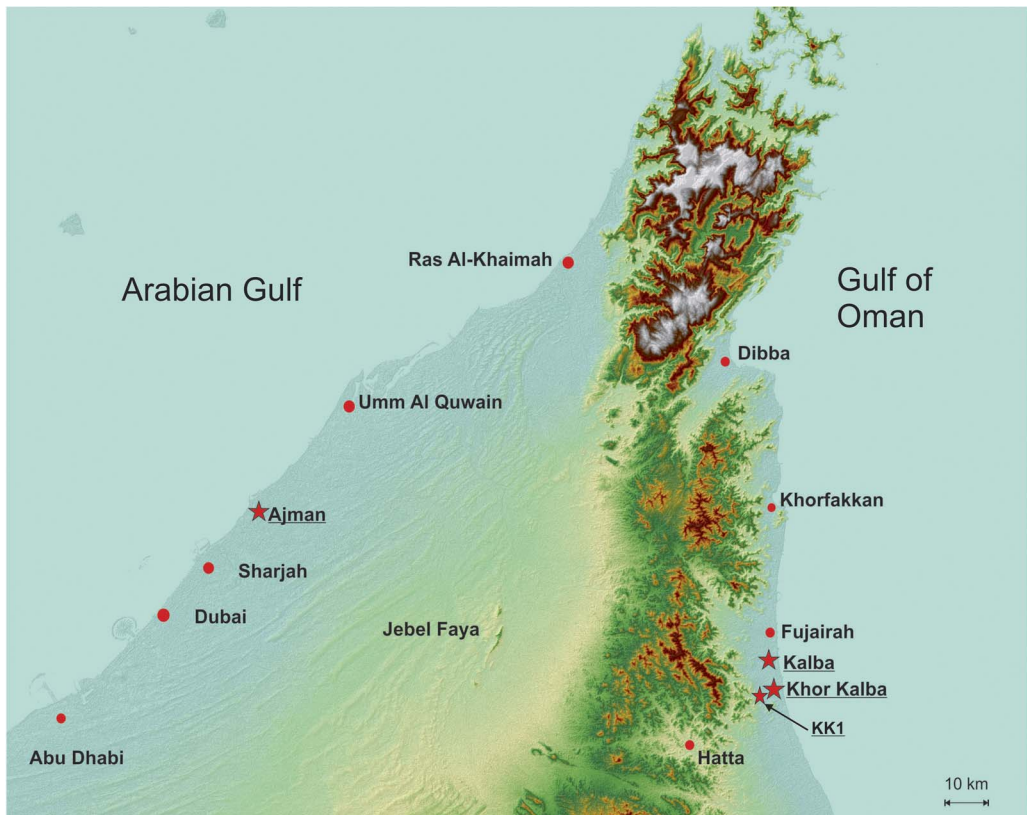


Figure 1 Map of southeast Arabia (United Arab Emirates). Sites mentioned in this publication are marked with a star and the text underlined.

time and differ among species and localities (Culleton et al. 2006). In Culleton's study, stable isotopes were used to trace influences of upwelling water as, for example, more intense upwelling is accompanied by higher  $\delta^{18}\text{O}$  values. These changes in stable isotopes reflect changes in environmental conditions like marine or terrestrial input. These changes are also mirrored in changes in the local reservoir ages. For the Arabian Peninsula, a systematic approach to understand the differences in reservoir ages has so far not been established for different species over different periods of time. Nevertheless, interesting and important work has been done on shells and mangroves with respect to archaeology and paleoclimate in Oman (Berger et al. 2005, 2013). In this article, we approach our research on the Gulf of Oman as a combination of stable isotope analyses,  $\delta^{13}\text{C}$ , and  $\delta^{18}\text{O}$ , to look for seasonal behavior in the shells as well as seawater or terrestrial input that will also influence the reservoir effect directly.

This article will take a closer look at two of the most abundant species in archaeological sites, the bivalve mollusk *Anadara uropigimelana* and the gastropod *Terebralia palustris*. Due to the differences of the molluscan lifestyle, we would expect minor differences in the reservoir age between *A. uropigimelana* and *T. palustris* from the same site. For example, *T. palustris* feeds on leaves, whereas *A. uropigimelana* feeds on plankton; hence, we would expect the *Terebralia* sp. to show a lower reservoir age than *Anadara* sp. due to the enhanced terrestrial signal in the food resource. However, owing to the upwelling of deep water in the Arabian Sea (Gulf of Oman), we expect a shift in reservoir age at the eastern coast of the Arabian Peninsula towards older ages.

The two mollusk species live in or near mangroves, places that were preferred environments for humans from where they gained most of their marine food. At first, we will concentrate on the Gulf of Oman, especially the region of Kalba, to study whether the shells usually found by archaeologists can also be used to for dating by tracing the reservoir age of (1) species and (2) seawater signature over time. Modern tree and sediment samples from Kalba and Ajman (Arabian Gulf) help to understand these complex systems and allow to trace back these patterns into the archaeological and paleoenvironmental context.

## Localities

### *Kalba*

Kalba is located in the Emirate Sharjah at the northern coast of the Gulf of Oman where the Hajar Mountains approach the coast (see Figure 1). Along the coast, mangroves are accompanied by *sabkhas* (coastal salt flats, former mangrove sediment) followed by gravel plains as well as wadi beds further inland (Phillips and Mosseri-Marlio 2002). Khor Kalba is the name of the region with few distinct settlement structures close to the sabkha and mangrove. The city Kalba itself lies north of the mangrove area (cf. Figure 1). Today, the large sabkha points to a more inland position—or an even wider extent—of the mangrove in earlier times (Phillips and Mosseri-Marlio 2002).

The oldest known shell midden of Kalba is situated along a hillslope of the Hajar Mountains at the western edge of the sabkha. During the excavations of Carl Phillips, this shell midden was referred to as KK1 (Khor Kalba site 1, Figures 1 and 7), which is the name we will use herein for consistency. The first hint towards a Neolithic age was derived from the bifacial stone tools found in the midden. These are indicative for the 5th millennium BC (Phillips and Mosseri-Marlio 2002). No archaeological settlement in the form of building remains has been found for this cultural period. One possible interpretation is that the midden represents a specialized area where mollusks were extracted, maybe also consumed, or packed for transport. The shell deposits of KK1 themselves are densely packed, covering a depth of roughly 50 cm. The majority of shells belong to the gastropod *T. palustris* and the oyster *Saccostraea cucullata* along with several specimens of the bivalve *Anadara* sp. The mangrove forest at Khor Kalba, with *Avicenna marina* as the dominant tree species, is today a protected natural area (Figure 2d).

### *Ajman*

Ajman lies north of Dubai and Sharjah at the coast of the Arabian Gulf. Today, a small mangrove and a lagoon are present. The environment around Ajman is arid with sand dunes in the outermost part of the Rub al-Khali. In contrast to Kalba, the mountains are more than 50 km away (cf. Figure 1). This has a direct influence on the freshwater input, with the input being lower in this area. The mangrove forest in Ajman was planted artificially around 10 yr ago most probably on a former mangrove sediment from ancient times. We chose to sample this mangrove only to gain insight into possible shifts in  $^{14}\text{C}$  age due to carbon pathways in the mangrove tree itself, here *Avicenna marina*, owing to the old sediment. Near Ajman, no settlement structure from the Neolithic with shell layers was accessible at the time of sampling.

### *Shells*

The gastropod *Terebralia palustris* (cf. Figure 2a) inhabits muddy sites of mangroves. Hence, it is also called a mud whelk or mud creeper. Its lifespan is currently unknown. The juvenile *T. palustris* spends its youth on the seaward front of the forests and moves deeper into the



Figure 2 Shell specimen from Khor Kalba referred to in this publication: (a) *Terebralia palustris*, (b) *Anadara uropigimelana*, (c) *Periglypta reticulata*, (d) Khor Kalba mangrove.

mangrove approximately at the age of four. It will thus have slightly different  $^{14}\text{C}$  signals (more depleted) as a young snail compared to adult snails. Therefore, no juvenile specimens are typically found in shell middens near mangroves (Pape et al. 2008). In addition, *T. palustris* changes its feeding habits during ontogeny. As a juvenile, it eats mud and fallen leaf debris, whereas the adult snail grazes on fallen leaves.

The bivalve *Anadara uropigimelana* (Figure 2b) lives in intertidal mudflats of lagoons and estuaries and reaches a lifespan of up to 45 yr (Petchey and Clark 2011). It can withstand large salinity fluctuations and lives at temperatures ranging between 15 and 32°C. The shell material is aragonite. *A. uropigimelana* is a surface deposit feeder and occurs throughout the Indian Ocean region (Tebano and Paulay 2000; Azzoug et al. 2012; Petchey et al. 2013). It buries itself in the sand up to a depth of 20 cm.

The bivalve *Periglypta reticulata* (see Figure 2c) can often be found in tropical environments such as the Indo-Pacific. It burrows in sand and mud of intertidal zones, but can also be found in sublittoral zones. It is a suspension feeder that subsists on planktonic algae and organic matter (Bieler et al. 2004). So far, no sclerochronological analyses have been performed



on *P. reticulata*, but it has a lifestyle and feeding habits similar to that of *Anadara* sp. We used *P. reticulata* to monitor the influence of the environment on shell growth because we did not find a live specimen of *A. uropigimelana*. It also allowed us to derive the sea surface temperature range for the mangrove at Khor Kalba.

### *Sclerochronology*

Bivalves and gastropods grow by periodically accreting carbonate at the shell margins. This results in distinct shell growth patterns consisting of growth lines and growth increments. Growth lines are formed during periods of slow growth, whereas growth increments represent periods of fast growth. Growth patterns can be used as an internal calendar to temporally align the growth record.

In intertidal settings, mollusks form growth patterns that closely reflect the tidal regime (House and Farrow 1968; Evans 1972; Ohno 1989; Schöne 2008). Growth lines are formed during low tide and growth increments during high tide. In semidiurnal tide regimes, a couplet of two (circatidal) increments and lines is thus developed, whereas in diurnal tidal regimes only one pair of a (circalunidian) increment and line is formed. During spring tides, the growth lines are more sharply delimited and more distinctly developed than during neap tides. This results in a distinct fortnightly (~14-day) growth pattern with bundles of ~13.5 (perigee fortnight cycle: new to full moon) and 15.5 (apogee fortnight cycle: full moon to new moon) circalunidian increments and lines, and 27 to 31 circatidal increments and lines (Hallmann et al. 2009). Note that the circatidal lines are typically much more pronounced than the semidiurnal growth patterns. Aside from tide-controlled growth patterns, there is also an annual slowdown of shell growth resulting in the formation of annual growth lines. Azzoug et al. (2012) hypothesize that their formation in *Anadara* sp. is controlled by harsh seasonal environmental conditions or the reproduction cycle.

Although some information is available on the food resources of the studied mollusk species and their interaction with the environment (Patel et al. 1978; Debenay et al. 1994; Azzoug et al. 2012), little is known about their growth histories. Azzoug et al. (2012) studied growth patterns and stable isotopes of *Anadara* sp. from Senegal to quantitatively estimate the duration of rainy and dry seasons and examine the possibility of using large fossil shell accumulations for studies of the long-term variability of the West African Monsoon seasonality. This formed the basis of our analysis of the same genus from the United Arab Emirates. For example, an increase in upwelling of seawater is accompanied by an increase in  $\delta^{18}\text{O}$  because colder deep water mixes with surface water. Estuarine inlets are more influenced by terrestrial runoff where streams are depleted in  $\delta^{13}\text{C}$  by 5–10‰ compared to mean ocean water. Freshwater inputs lower both  $\delta^{13}\text{C}$  and  $\delta^{18}\text{O}$  (Culleton et al. 2006). These effects should also be mirrored as small changes in the local reservoir effect and provide information on the sources of these changes.

## **MATERIALS AND METHODS**

### **Sampling Strategy**

As the mangrove in Kalba (Figure 2d) existed for several thousand years and survived many generations of trees, it is an ideal sampling site for our study. To determine the reservoir age of *A. uropigimelana* and *T. palustris*, we sampled a shell midden (KK1) at Khor Kalba, Gulf of Oman (Figure 1 and Table 1). We used a trench from an earlier excavation with a distinct ash layer close to the bottom (see Figure 7). As it was not clear at the beginning whether all the shells

Table 1 Samples taken at Khor Kalba shell midden KK1.

Lab code	Sample name	Site	Material	Remarks
MAMS 22875	KSM BL Ash	Kalba KK1	Ashy sediment	Ash layer
MAMS 22876	KSM BL Terebralia	Kalba KK1	Shell marine	In ash layer
MAMS 22877	KSM UBL Terebralia	Kalba KK1	Shell marine	Below ash
MAMS 22878	KSM UBL Anadara	Kalba KK1	Shell marine	Below ash
MAMS 22879	KSM OBL Terebralia	Kalba KK1	Shell marine	Above ash
MAMS 22880	KSM OBL Anadara 1	Kalba KK1	Shell marine	Above ash
MAMS 22867	KSM OBL Anadara 2	Kalba KK1	Shell marine	Above ash
MAMS 22884	KSM 10-15 Terebralia	Kalba KK1	Shell marine	10–15 cm below surface
MAMS 22885	KSM 10-15 Anadara	Kalba KK1	Shell marine	10–15 cm below surface
MAMS 22882	KSM GOF Terebralia	Kalba KK1	Shell marine	Just below surface
MAMS 22883	KSM GOF Anadara	Kalba KK1	Shell marine	Just below surface

would give the same age or whether age differences existed following the stratigraphic order, we sampled several shell layers (Table 1). We expected to find two distinct age ranges around 4000 BC for shell midden KK1 based on the excavation Phillips and Mosseri-Marlio (2002). Unfortunately, the ash layer contained only tinsels of charcoal in a sandy matrix instead of distinct charcoal fragments. Being close to the mangrove, it seemed obvious that one source of wood might be the mangrove itself. The dominant mangrove tree in Kalba today is *Avicenna marina*. When we derive a reservoir effect for the shells from paired terrestrial-marine samples, we must be sure to understand the terrestrial samples as well. With the hypothesis that the main source of the carbon in the ash is burnt mangrove tree, we sampled modern leaves and branches together with the first few cm of sediment in the Mangrove at Kalba (protected area, see Figure 2d and Table 2). Even without measuring the sediment with respect to its compounds, it allows an interpretation of the data of the trees. Understanding this system is crucial not only to characterize the signal of the ash in case it was mainly wood from *Avicenna* sp., but also because the leaves provide a food resource for the mollusks. If the tree incorporates old carbon from the sediment in significant amounts, its terrestrial signal is in fact a mixed signal and could not be used for determining a reservoir effect.

We also sampled the mangrove at Ajman, Arabian Gulf (Figure 1, Table 2). However, as the mangrove at Ajman was planted 10 yr ago on the sediment of a former mangrove sabkha, we used it to trace carbon pathways in the mangrove tree that might influence molluscan specimen using mangrove leaves as the food resource.

Shells have been successfully used as tracers of environmental and climate changes (Rollins et al. 1990; Schöne et al. 2005b; Wanamaker Jr et al. 2011; Azzoug et al. 2012; Marali and Schöne 2015). Therefore, we took a closer look at *A. uropigimelana* shells and the single specimen of *P. reticulata* in order to analyze their potential use as environmental recorders for the lagoonal setting. *P. reticulata* was chosen as no modern *Anadara* sp. could be found. In this study, *T. palustris* was not used for the sclerochronological analysis part, but will be studied in the near future. The reservoir effect is a mirror for environmental influences and these are recorded in the shell. Knowledge about how fast a mollusk reacts to its environment and at what time it builds the shell (throughout the year at the same rate or rather seasonal), and hence records the changes, is important to know if we want to use it later as a paleoclimate indicator (not in this paper).

Table 2 Samples taken at the mangroves of Ajman (Arabian Gulf) and Khor Kalba (Gulf of Oman).

Lab code	Sample name	Site	Material
MAMS 21281	AM1 leaf	Ajman mangrove	Leaf
MAMS 21282	AM2 branch	Ajman mangrove	Wood
MAMS 21283	AM3 sediment	Ajman mangrove	Sediment
MAMS 21270	KNR1 leaf	Kalba mangrove	Leaf
MAMS 21271	KNR2 branch	Kalba mangrove	Wood
MAMS 21274	KNR3 sediment	Kalba mangrove	Sediment
MAMS 22868	KS M1 <i>Periglypta</i>	Kalba mangrove entrance	Shell marine

### Sclerochronology of *Anadara* sp. and *Periglypta* sp.

To prepare the bivalve specimens for sclerochronological analyses, i.e. growth pattern and stable isotope analyses ( $\delta^{13}\text{C}$  and  $\delta^{18}\text{O}$ ), the shells are mounted to a Plexiglass block with a quick-drying plastic welder. Two ~3 mm-thick sections were cut from within each shell along the axis of maximum growth perpendicular to the annual growth line using a Buehler Isomet 1000 low-speed precision saw equipped with a 0.4-mm-thick diamond wafering blade. Then, the sections were mounted on glass slides, ground with SiC (800 and 1200 grit), and polished with  $\text{Al}_2\text{O}_3$  powder (1  $\mu\text{m}$ ). Between each step, the sections were ultrasonically rinsed (Schöne et al. 2011). One of the two (air-dried) sections was used to study annual growth patterns. For this purpose, the polished section was immersed in Mutvei's solution for 20 min at 37–40°C (Schöne et al. 2005a), then rinsed with demineralized water and air-dried. Mutvei's solution facilitates the recognition of shell growth patterns as it stains growth lines dark blue and produces a three-dimensional relief of etch-resistant growth lines and deeply etched growth increments. The growth patterns were then viewed under a reflected-light stereomicroscope (Leica Wild M2C) and digitized with a Nikon Coolpix 995 camera. Increment widths were measured using the software Panopea (©Schöne and Peinl).

To determine the possible relationship between shell growth rate and increment width of the *Anadara* sp. and *Periglypta* sp., inherent age-related growth trends were first mathematically eliminated. This was accomplished by fitting a polynomial function to the growth curve and computing dimensionless growth indices (Schöne and Surge 2012) by calculating the ratio of the measured versus predicted growth value at each year. Subsequently, these values were standardized in order to directly compare relative growth increment time series of different individuals with each other or with environmental variables.

The other polished shell section (second slice of the valve) of the *A. uropigimelana* specimen was first inspected via Raman spectrometry to determine the  $\text{CaCO}_3$  polymorph. Raman measurements were done at the Institute of Geosciences at the University of Mainz (Horiba Jobin Yvon LabRam 800 spectrometer equipped with Olympus BX41 optical microscope); for further details, see Milano et al. (2015). Then, powder samples for stable isotope analysis were drilled or milled from the shell of both species following the growth pattern by using a cylindrical diamond drill bit (1 mm diameter, Komet/Gebr. Brasseler GmbH and Co. KG model no. 835104010) mounted to a Rexim Minimo drill system. Samples (50–120  $\mu\text{g}$ ) were analyzed with a Finnigan MAT 253 continuous-flow isotope ratio mass spectrometer equipped with a Gas Bench II. Isotope values were reported relative to V-PDB and calibrated against a Carrara marble standard ( $\delta^{18}\text{O} = -1.91\text{‰}$ ;  $\delta^{13}\text{C} = 2.01\text{‰}$ ). The precision error based on repeated

measurements of the standards is better than  $\pm 0.07\text{‰}$  for  $\delta^{18}\text{O}$  and better than  $\pm 0.05\text{‰}$  for  $\delta^{13}\text{C}$ . For more details of the measurement procedure, see Füllenbach et al. (2015).

First, we sampled the shells by drilling holes in the outer shell layer at nearly equidistant intervals. To obtain a higher resolved isotope time series, a 4-mm portion of the *Anadara* sp. shell was micromilled in steps of  $\sim 100\ \mu\text{m}$  parallel to the growth lines (Figure 4). These samples were used to determine  $\delta^{18}\text{O}$  and  $\delta^{13}\text{C}$  values. Shell growth patterns were used to temporally contextualize the isotope data, i.e. to assign seasonal dates to the sampled shell portions. Because of the lack of modern *Anadara* sp. during our sampling campaign, we chose to use another bivalve, *P. reticulata*, to trace changes in environment, here water temperature reflected in the  $\delta^{18}\text{O}$  signal, in this estuarine habitat as well as response time of the shell species. Being similar to *Anadara* sp. in food resources and habitat, this allows to draw some conclusions for both species.

### Preparation of Radiocarbon Samples and the Reservoir Effect

Samples for  $^{14}\text{C}$  dating were prepared at the Klaus-Tschira-Archaeometry Centre, Mannheim. To determine the  $^{14}\text{C}$  data close to the time when the mollusks died, if possible the most recently formed shell material was used, i.e. the ventral margin in the case of the bivalves and the aperture or last visible whorl in the case of the gastropods. From the ventral margin, small chips were taken and surface contamination, such as sedimentary calcium carbonate removed by etching the fragments in 1% HCl in an ultrasonic bath for 1 min. All information on the concentration of the chemicals used here refers to vol % if not mentioned otherwise. The ultrasonic bath provides a soft mechanical treatment during the etching process. Next, the fragments were rinsed in distilled water and dried.

We determined the local reservoir age for the Khor Kalba mollusk samples (*A. uropigimelana* and *T. palustris*) from the shell midden as paired samples in connection with the ash layer (containing about 5% C) in which they were embedded, which we interpret as being contemporaneous. Although ash contains a lot of siliceous material, it shows tinsels of charcoal, which we extracted by floating; hence, we are sure to be able to use it like charcoal. The ashy sediment sample, containing a large amount of carbonate, was etched with 4% HCl (hydrochloric acid) for several hours in order to completely remove remnants of sedimentary  $\text{CaCO}_3$ . When the reaction stopped, the acid was changed until no carbonate reaction was recognized. This step was undertaken at room temperature. Subsequently, the sample was treated with 0.4% NaOH (sodium hydroxide) to remove humic acids. Finally, the sample was treated again with 4% HCl at  $60^\circ\text{C}$ . The mangrove samples (leaves and branches to check for possible reservoirs effects in the tree) from Khor Kalba and Ajman, were treated with acid-base-acid (ABA)—4% HCl, 0.4% NaOH, and again 4% HCl at  $60^\circ\text{C}$ —to remove carbonates and surface contamination. The sediment samples from the mangrove soil experienced a treatment comparable to the ash sample with two steps of 4% HCl and a step using 0.4% NaOH in between to remove any carbonates and humic acids, respectively. Between each step and after the entire pretreatment, samples were rinsed with distilled water and finally dried at  $60^\circ\text{C}$ . The terrestrial samples (ash, leaves, branches, sediments) were combusted using an elemental analyzer (Micro Cube, Elementar) as described in (Lindauer and Kromer 2013). The shell samples were converted to  $\text{CO}_2$  using phosphoric acid in an Autosampler system at  $70^\circ\text{C}$  as described in Wacker et al. (2013) and graphitized with the AGE III system, both produced by Ionplus (Switzerland). All graphite samples were measured at the DatingMicadas in Mannheim and corrected for isotopic fractionation as described previously (Kromer et al. 2013; Lindauer and Kromer 2013).



The reservoir effect was calculated as the difference between the two archives using the software package ResAge by Guillaume Soulet (2015), which can be downloaded as a supplement to his publication.

## RESULTS AND DISCUSSION

### Sclerochronology and Stable Isotopes

#### *A. uropigimelana* from Shell Midden KK1

The growth patterns of the *A. uropigimelana* specimen from the shell midden KK1 were difficult to determine. Immersion in Mutvei's solution only resulted in a pale blue-colored surface, so that the growth increments and lines were hard to recognize. Eventually, a diagenetic overprint resulted in a loss of some organic matrices, which the dye contained in Mutvei's solution, Alcian Blue, would typically stain. However, diagenetic alteration was not more severe. As demonstrated by Raman spectrometry, the examined old shell still consists of aragonite and has not been converted into calcite (Figure 3).

Due to the difficulties with the Mutvei's solution, we chose to count only the most distinct growth lines (Figure 4). The width of the annual increments decrease through ontogeny, representing the well-known age trend (von Bertalanffy 1938; Jones et al. 1989; Azzoug et al. 2012; Marali and Schöne 2015). The seasonal temporal alignment of the shell record, and thus the rate of seasonal shell formation, was accomplished by comparing the  $\delta^{18}\text{O}$  curve with the growth patterns. As can be seen in Figure 4, the  $\delta^{18}\text{O}$  curve (blue line) shows a clear sinusoidal shape, which can be interpreted as a seasonal temperature signal. It also shows that the growth increments not only represent annual lines, but are superimposed by distinct growth marks probably caused by changes in food resource or escape from predators (stress mark). Since shell oxygen isotope data and temperature are negatively correlated (Grossman and Ku 1986; a change in  $\delta^{18}\text{O}$  by 1‰ corresponds to a change in water temperature of  $\sim 4.3^\circ\text{C}$ ), more positive  $\delta^{18}\text{O}$  values indicate colder water temperature and more negative  $\delta^{18}\text{O}$  values warmer water. In the studied specimen,  $\delta^{18}\text{O}$  values slowly increased after the annual growth line, followed by

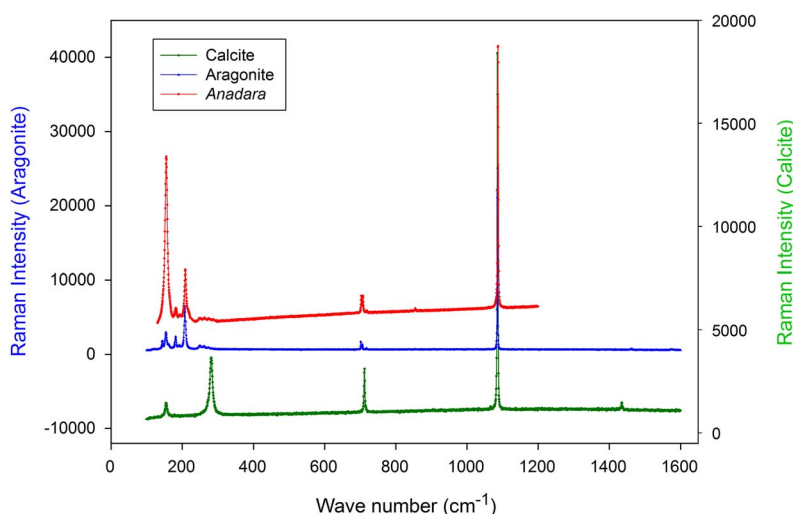


Figure 3 Raman spectroscopy of one *A. uropigimelana* specimen (top line) and the carbonate reference materials (pure calcite is the bottom line; pure aragonite is shown in between the sample and the calcite data).

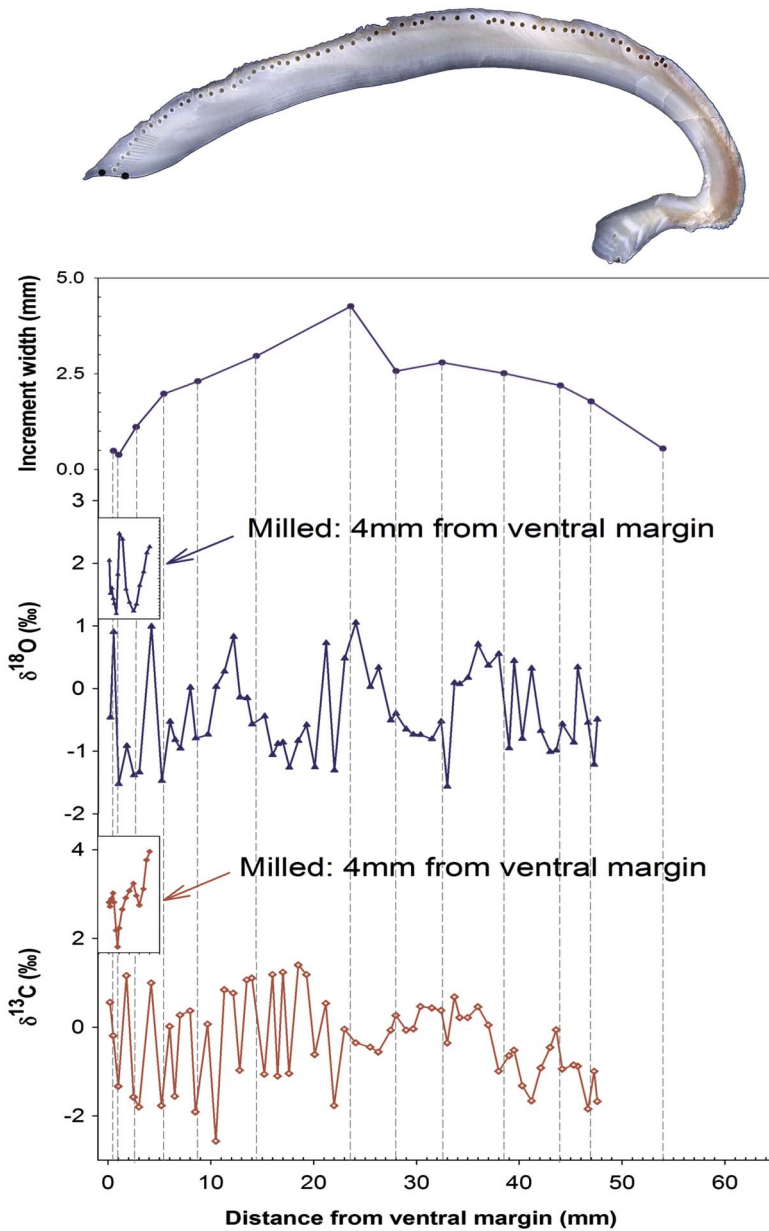


Figure 4 Polished section of *Anadara uropigimelana* (MAMS 22867) from Khor Kalba shell midden KK1 on top. The holes originate from drilling the samples. Displayed below are the results of the growth increment width (top);  $\delta^{18}\text{O}$  and  $\delta^{13}\text{C}$  values from powder samples obtained via drilling are represented as triangles (middle) and diamonds (bottom), respectively. Insets display stable isotope data from milled powder samples. DOG denotes direction of growth.

a more rapid decrease toward the following annual growth line. These findings suggest that the shell grew more rapidly during the winter season than during summer, and the annual growth line formed during the warmest season. The studied specimen died during winter.

Interpreting the  $\delta^{13}\text{C}$  signal is very challenging. Besides a strong physiological control, the stable carbon isotopes reflect changes in food availability, the water dissolved inorganic carbon (DIC) signature, and freshwater input (Khim et al. 2003; Culleton et al. 2006). Generally speaking, it can be said that strong freshwater input results in a depletion of  $\delta^{13}\text{C}$  due to soil processes and plant material. The signal of  $\delta^{18}\text{O}$  also decreases in a similar way because of fractionation during precipitation and reduced salinity of the freshwater. For the same reasons, the apparent  $^{14}\text{C}$  age and the local reservoir effect could increase.

The  $\delta^{13}\text{C}$  signal rises slowly and oscillates around a constant value with some distinct features. Towards the ventral margin, drilling obviously cannot resolve the patterns properly in contrast to milling the sample section. The pattern of  $\delta^{13}\text{C}$  resembles that of the  $\delta^{18}\text{O}$  curve with respect to positions of minimal and maximal values at several points. From the wider shape of the features in both curves, it can be inferred that the *Anadara uropigimelana* specimen grew up in a more homogeneous environment and later moved closer to the mangrove with multiple changes in food resources, freshwater, and water temperature.

#### *Periglypta reticulata* and Modern Lagoonal Signal

To investigate the extent to which shells from a lagoon also reflect seasonal patterns in  $\delta^{18}\text{O}$  and  $\delta^{13}\text{C}$ , a modern sample of *P. reticulata* from Kalba, which shows similar lifestyle and feeding behavior as *Anadara* sp., was analyzed. As demonstrated in Figure 5, distinct seasonal and subseasonal growth lines and increments are developed in *P. reticulata* shells. Subseasonal growth patterns seem to be controlled by the tides because they show a recurrent pattern of about 13 to 15 lines and increments, possibly reflecting circlunidian growth patterns. Altogether, more than 580 microgrowth lines were counted in a shell portion that likely formed during 2 yr. This further supports the interpretation of lunar daily growth patterns.

Judging from the  $\delta^{18}\text{O}$  curve, the studied shell portion was formed during a time interval of ~2 to 3 yr (compare Figure 6). The shell was collected in December 2013 with closed valves but without a mollusk inside. When interpreting the last point of the graph in Figure 6 as being very close to the time of death, it becomes evident that the shell died in winter. The  $^{14}\text{C}$  measurement allows us to interpret that it died shortly before it was collected, although with a second possible result around 1956. The  $\delta^{18}\text{O}$  values at the ventral margin show very high positive values,



Figure 5 *Periglypta reticulata*, Khor Kalba (MAMS 22868), excerpt of section etched with Mutvei's solution for growth increment analysis.

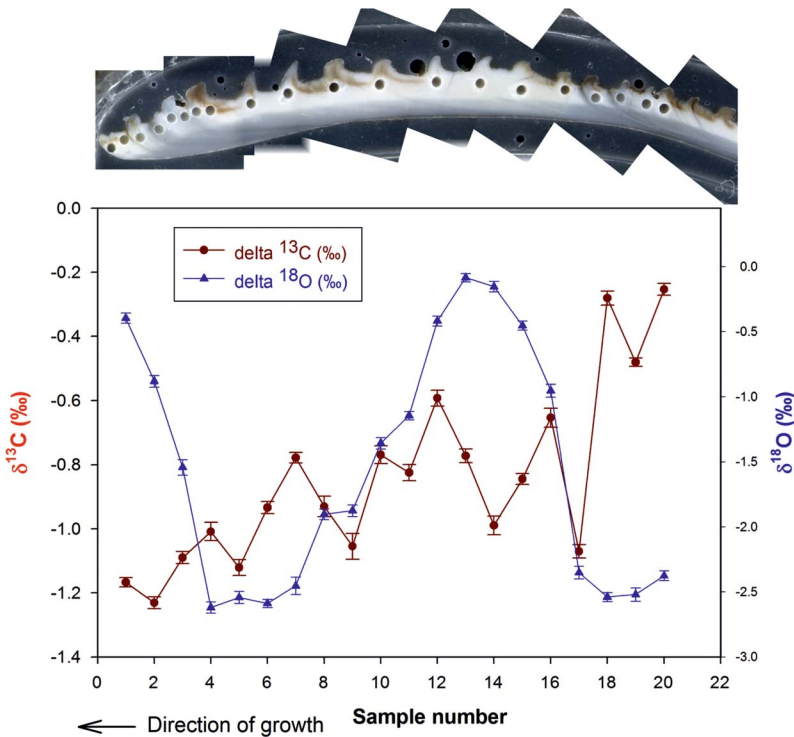


Figure 6  $\delta^{18}\text{O}$  (triangles, sinusoidal line) and  $\delta^{13}\text{C}$  (dots) measurements of *Periglypta reticulata* shell from Khor Kalba. On top the polished section with the drilled sample locations can be seen. “DOG” denotes direction of growth.

which suggest cold temperatures. Like *A. uropigimelana*, *P. reticulata* seems to grow at maximum rate during the colder months of the year (winter and spring), whereas shell formation rate is reduced during summer (minimum  $\delta^{18}\text{O}$  values). Therefore, the species *P. reticulata* seems to react immediately on changes in water temperature reflected in the  $\delta^{18}\text{O}$  signal.

*P. reticulata* with a change in  $\delta^{18}\text{O}$  of up to 2.5–3‰ allows us to interpret traceable environmental changes in the lagoon throughout the year reflected in water temperature changes of 12–16°C. As mentioned earlier and quoted from Grossman and Ku (1986), a change in  $\delta^{18}\text{O}$  by 1‰ corresponds to a change in water temperature of 4.3°C. The  $\delta^{13}\text{C}$  pattern is following a certain trend towards more negative values. There seems to be a parallel trend with  $\delta^{18}\text{O}$  between samples 8 and 12 during the maximum growth period between winter and spring that points to a depletion of both signals, probably influenced by freshwater. The parallel rise of both stable isotope signals towards positive values around sample 17 might originate from some change in the signal of the food resource as it coincides with two distinct growth marks. Thus, also the  $\delta^{13}\text{C}$  influences are recorded rather quickly in the shell. We see here that this estuarine habitat shows clear seasonal changes and the bivalves (*Anadara* sp. as well as *Periglypta* sp.), although they bury in the sediment, record these changes in their shell.

#### Radiocarbon Dating and Reservoir Age

For the shell midden KK1 at Kalba, we found two age groups corresponding to around 6900 and 6300 BP (Table 3, Figure 7), which point to two distinct layers of the shell midden as



Table 3 Results of  $^{14}\text{C}$  measurements on the samples from the shell midden KK1, Khor Kalba. Refer to Table 1 for sample description.

Lab code	Sample name	$^{14}\text{C}$ (BP)	F $^{14}\text{C}$
MAMS 22875	KSM BL Ash	6117 $\pm$ 26	0.4670 $\pm$ 0.0015
MAMS 22876	KSM BL Ter	6911 $\pm$ 28	0.4230 $\pm$ 0.0015
MAMS 22877	KSM UBL Ter	6924 $\pm$ 27	0.4224 $\pm$ 0.0014
MAMS 22878	KSM UBL Ana	7058 $\pm$ 27	0.4153 $\pm$ 0.0014
MAMS 22879	KSM OBL Ter	6545 $\pm$ 26	0.4427 $\pm$ 0.0014
MAMS 22880	KSM OBL Ana	6273 $\pm$ 27	0.4580 $\pm$ 0.0015
MAMS 22882	KSM MuGOF Ter	6257 $\pm$ 26	0.4589 $\pm$ 0.0015
MAMS 22883	KSM MuGOF Ana	6310 $\pm$ 26	0.4559 $\pm$ 0.0015
MAMS 22884	KSM 10-15 uGOF Ter	6262 $\pm$ 26	0.4586 $\pm$ 0.0015
MAMS 22885	KSM 10-15 uGOF Ana	6272 $\pm$ 27	0.4580 $\pm$ 0.0015
MAMS 22867	KSM A2OBL Ana	6295 $\pm$ 26	0.4567 $\pm$ 0.0015

proposed by Phillips and Mosseri-Marlio (2002). In order to calculate a preliminary local reservoir age for this period at Kalba, we used samples from the lowermost layer containing the ashy sediment (Table 4). We call it preliminary as the shell midden needs further sampling of shells to establish the statistical significance. The thorough pretreatment of the ash samples resulted in a reliable age of  $6117 \pm 26$  yr BP. The program ResAge was applied to the  $^{14}\text{C}$  data of the ash and shells collected from the same layer (see Table 1). For the two *T. palustris* specimens, we received reservoir ages of 794 and 807 yr and calculated a simple mean value of 800.5 yr for the Neolithic period at Kalba for this species, being aware of the lack of statistical significance. There seems to be a difference from the local reservoir effect of *A. uropigimelana*, which was even higher than the one for *T. palustris*, namely  $941 \pm 37$  yr older than the contemporaneous ash. One could argue that the shell might be older because of a really older age than the charcoal in the ash, but then also the *Terebralia* of the same layer should be much older. In the lowermost layer, hardly any *Anadara* sp. were found, which we interpret as being the time when it started to settle at Khor Kalba and only few specimens were caught by fishermen. This reservoir age, too, is preliminary and needs further sampling. Although we did not use a statistically significant amount of shells per species, we can say that the local reservoir age for Kalba at this period is higher than the reservoir effects we find in the literature cited in the Introduction, and indeed differs between the species under investigation. Looking at the values in Southon et al. (2002), we see that for some species the authors find few values from the 19th century that are not too different with  $786 \pm 51$   $^{14}\text{C}$  yr BP (*Marcia flammea* from Muscat). The ash sample was also measured with an IRMS in Mainz to determine its  $\delta^{13}\text{C}$  value. With a  $\delta^{13}\text{C}$  of  $-25.76\text{‰}$ , we can say that the ash sample extracted consisted of charcoal from wood (mangroves lie in the range of  $-24$  to  $-28$  for leaves, see Rodelli et al. 1984).

The modern leaf, wood, and sediment samples from the mangroves at Ajman and Kalba showed the contributions of atmosphere and dead carbon on the mangrove  $^{14}\text{C}$  data (Table 5): sediments from the artificially planted mangrove at Ajman (Arabian Gulf) yield an age of 2200 yr BP, and also the branch and the attached fresh leaf were a lot older than expected, resulting in a collection year of around AD 1955 instead of AD 2013. This suggests that the plants incorporated carbon from the sediment as well as from the atmosphere. The reservoir effect at Kalba is less pronounced with sediment ages of 620 yr BP. At Kalba, the mangrove itself, leaves, and wood, show a shift in age of 2 yr (estimated) and point to a time of collection

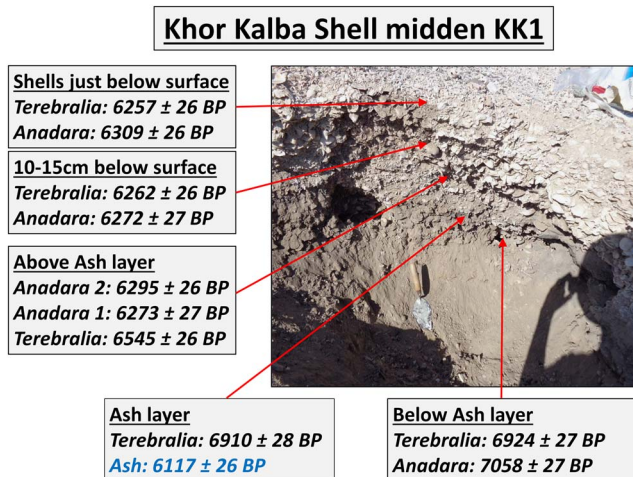


Figure 7 Khor Kalba shell midden KK1 and uncalibrated data from radiocarbon measurements of different depth in the stratigraphy. The age of the terrestrial sample (“ash”) is written in blue-gray.

Table 4 Radiocarbon local reservoir effect of *T. palustris* (including mean value) and *A. uropigimelana* from Khor Kalba. The corresponding stratigraphy of the shell data can be seen in Figure 8. The  $\delta^{13}\text{C}$  for the ash sample was measured with an IRMS.

Lab code	Sample	F <sup>14</sup> C	R(t)	R(t), mean	Remarks
MAMS 22875	KSM BL Ash	0.4670 ± 0.0015			$\delta^{13}\text{C} = -25.76\text{‰}$
MAMS 22876	KSM BL Ter	0.4230 ± 0.0015	794 ± 38	800.5 ± 53	Mean R(t) only
MAMS 22877	KSM UBL Ter	0.4224 ± 0.0014	807 ± 37		on <i>T. palustris</i> , 1 $\sigma$
MAMS 22878	KSM UBL Ana	0.4153 ± 0.0014	941 ± 37		

Table 5 Radiocarbon measurements of Mangrove samples from Ajman (AM), Kalba natural reservation area (KNR) and the *Periglypta reticulata* specimen from Kalba beach.

Lab code	Sample name	F <sup>14</sup> C	<sup>14</sup> C (BP)
MAMS 21281	AM 1 plant	1.0106 ± 0.0023	
MAMS 21282	AM2 wood	1.0128 ± 0.0023	
MAMS 21283	AM3 sed	0.7599 ± 0.0018	2205 ± 19
MAMS 21270	KNR1 leaf	1.0274 ± 0.0023	
MAMS 21271	KNR2 wood	1.0314 ± 0.0023	
MAMS 21274	KNR 3 sed	0.9255 ± 0.0021	620 ± 18
MAMS 22868	KS M1T2 <i>Periglypta</i>	1.0220 ± 0.0025	

approximately 2011 to 2013 (Figure 8). Here, we can derive a negligible influence of sediment on which the mangrove grows. Overall, the reservoir effect on the mangrove wood itself is insignificant for determination of the reservoir age of the shells and does allow the calibration of mangrove data as terrestrial material. Regarding the pathways, we see the fresh leaves essentially influenced by the atmosphere. For the mangrove wood, in fact the branch on which the leaf was attached, this is also true although it shows a little older age, which just reflects that it started to grow longer ago than the leaf. The crucial role of the samples from Ajman here lies

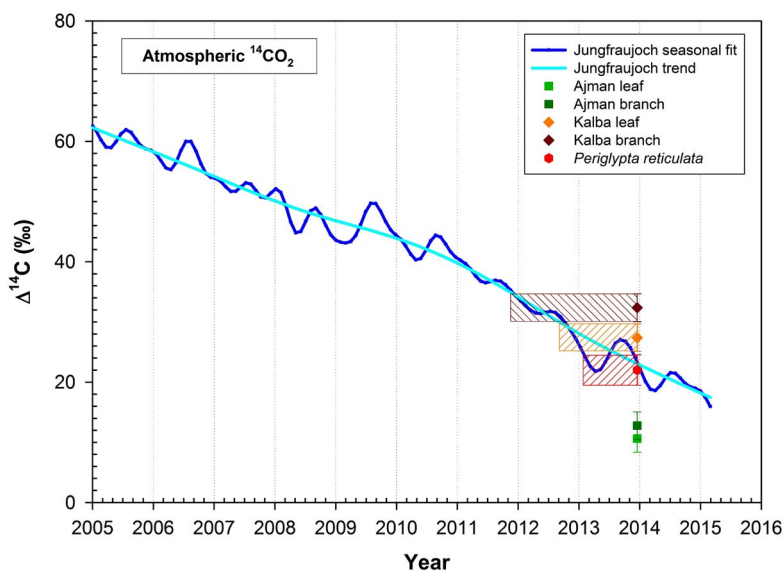


Figure 8 Modern samples of Mangroves Ajman and Kalba (data cf. Table 5) in comparison with atmospheric data from Jungfrauoch, kindly provided by Ingeborg Levin (unpublished data).

in the fact that the trees were planted on a carbonaceous soil (old sabkha), which is responsible for the larger deviation from the expected result and hence a more obvious reservoir effect. We can thus say that maybe up to 1‰ of dead carbon (1‰ corresponds to ~80  $^{14}\text{C}$  yr) can be incorporated in the trees.

When calibrating the modern bomb  $^{14}\text{C}$  samples to check their correspondence with the time of collection in December 2013, using the software CALIBomb (<http://calib.qub.ac.uk/CALIBomb/>), we only received periods corresponding to around 1955. Ingeborg Levin kindly provided us the new atmospheric  $^{14}\text{C}$  measurements from Jungfrauoch (Switzerland) to test whether the modern samples might have corresponding intersections on the atmospheric curve. For the leaf and wood samples from Ajman, we received no intercept after 1955. However, at Kalba (Gulf of Oman) we found a corresponding intercept for leaf and wood samples as well as the *P. reticulata* shell within the last 2 yr since collection in December 2013 (Figure 8, in addition to the intercepts around 1955). Our modern shell, *P. reticulata*, even seemed to have very little or no reservoir effect, which is rather unexpected. Of course, a second possible result occurs in the 1950s. This interpretation must be taken with caution because the atmospheric measurements were not done on the Arabian Peninsula and due to the meridional gradient the  $^{14}\text{CO}_2$  level might be 1–2‰ higher than at the Jungfrauoch station in Switzerland (I Levin, personal communication). But without any contemporary atmospheric data from this area, this allows us to at least estimate any shifts. Moreover, this species has not yet been in the focus of research with respect to sclerochronology and  $^{14}\text{C}$  reservoir effects.

## CONCLUSIONS

The measurements on modern mangroves from both coastal regimes point to a minor influence of the sediment on the tree data, which is expected even when taking the atmospheric influence on leaves and aerial roots of *Avicenna marina* into account. We were able to show that both

species *A. uropigimelana* and *T. palustris* are suitable for determining the local reservoir effect, and in the case of *A. uropigimelana*, to provide information on the environmental conditions in which they lived using the light stable isotopes  $\delta^{13}\text{C}$  and  $\delta^{18}\text{O}$ . For *T. palustris*, the latter still needs to be verified for the study area. The modern sample of the mollusk *P. reticulata* was useful to calibrate the life history of this species and monitor the rate of change in water temperature of the estuarine at Khor Kalba.

Our measurements suggest a difference in reservoir age between both species of roughly 100 yr with *A. uropigimelana* pointing to a higher local reservoir effect during the Neolithic period. These rather high values for the reservoir ages point to either a period of stronger upwelling of ocean water from the Arabian Sea or strong freshwater input if the freshwater feeding the mangrove should be depleted in  $^{14}\text{C}$ , which has not been investigated so far. Our reservoir ages of 800 and 940 yr are certainly higher than those derived by Zazzo et al. (2012, 2016) who quote a mean value of  $645 \pm 40$  yr (4th millennium BC) for *Anadara antiquate* and  $568 \pm 56$  yr (5th millennium BC) for a mixture between several species in Ras al-Hamra, Oman, but our findings seem to be consistent with the *Marcia flammea* specimen from Muscat ( $786 \pm 51$  yr BP) quoted in Southon et al. (2002). This can be explained by the locations of the two sites. Kalba is further north towards the Strait of Hormuz where the Oman Sea tightens up, whereas in Ras al-Hamra and Muscat the Oman Sea is a lot more open and part of the Arabian Sea; hence, it might have a slightly different local circulation pattern. The difference between the species clearly reflects the differences in food resource and habitat, leaves compared to plankton and attaching to roots compared to burying in the sand. The isotope data of the prehistoric shell showed a more erratic signature of the stable isotopes than the modern specimen. This might be due to differences in oceanic circulation or terrestrial influences, but might also reflect changes in microstructures due to the age of the specimen. Additionally, the *Anadara* sp. shell covered roughly 6 yr where the *Periglypta* sp. shell with the same size covered only about 2–3 yr and hence provided a higher resolution. It would be helpful to investigate the fluctuations in  $^{14}\text{C}$  at the same positions where the stable isotope measurements had been sampled. This would help to interpret the origin of the signal, probably also for  $\delta^{13}\text{C}$  and allow to deduce the possible variability of the reservoir age over the shells lifetime. Hence, archaeologists trying to interpret data on the basis of shell measurements should ensure to use a species that has been investigated with respect to this problem or discuss the data according to the aspects presented here. We need to draw our attention to changes in local reservoir age over time and monitor changes, e.g. during the Bronze Age, to provide the archaeologists with the appropriate reservoir age.

The systematic approach to understanding the correlation between atmospheric and marine signal in the shells but also in their food resource and habitat turned out to be the ideal basis for determining and understanding the local reservoir age on the two species under investigation, *T. palustris* and *A. uropigimelana*. The stable isotope measurements allow to derive seasonality, changes in habitat, and response time for environmental changes to explain changes of the reservoir age over the shells lifetime as well as changes over different periods in time. In a next step, we will extend this research to a different period that is important for the archaeologists as well (Bronze Age, Iron Age). An important topic of future work will be the stable isotope analysis on *T. palustris*, to not only to determine the lifespan of this species and to what extent it mirrors environmental changes, e.g. fluctuations of salinity, sea surface temperature ( $\delta^{18}\text{O}$ ), or food resources ( $\delta^{13}\text{C}$ ). This would provide necessary information for archaeologists and paleoclimatology. Being able to derive reservoir effects with the same species enables tracing environmental changes through changes in the reservoir effects.



## ACKNOWLEDGMENTS

The authors would like to thank Dr Sabah Jasim and Eisa Yousif from the Department of Antiquities Sharjah for the possibility to work in this area. We are much obliged to the Environment & Protected Areas Authority of the Government of Sharjah for admission to the protected mangrove in Khor Kalba. Dr Ingeborg Levin, Institute for Environmental Physics, Heidelberg, kindly provided atmospheric  $^{14}\text{C}$  data. Michael Maus, Institute for Geosciences, Mainz, was a great help in running the stable isotope measurements. We are very grateful to Dr Tobias Häger, Dr Amy Prendergast, and Stefania Milano, Institute for Geosciences, Mainz, for performing the Raman spectrometry.  $^{14}\text{C}$  and stable isotope measurements were financed by Deutsche Forschungsgemeinschaft (DFG HI 643/23). Moreover, we would like to thank the two reviewers for their help with improving the manuscript.

## REFERENCES

- Armitage SJ, Jasim SA, Marks AE, Parker AG, Usik VI, Uerpmann H-P. 2011. The southern route 'out of Africa': evidence for an early expansion of modern humans into Arabia. *Science* 331(6016):453–6.
- Azzoug M, Carré M, Schauer AJ. 2012. Reconstructing the duration of the West African Monsoon season from growth patterns and isotopic signals of shells of *Anadara senilis* (Saloum Delta, Senegal). *Palaeogeography, Palaeoclimatology, Palaeoecology* 346–347:145–52.
- Berger JF, Cleuziou S, Davtian G, Cattani M, Cavulli F, Charpentier V, Cremaschi M, Giraud J, Marquis P, Martin C, Méry S, Plaziat JC, Saliège JF. 2005. Évolution paléogéographique du Ja'alan (Oman) à l'Holocène moyen: impact sur l'évolution des paléomilieux littoraux et les stratégies d'adaptation des communautés humaines. *Paléorient* 31(1): 46–63.
- Berger JF, Charpentier V, Crassard R, Martin C, Davtian G, López-Sáez JA. 2013. The dynamics of mangrove ecosystems, changes in sea level and the strategies of Neolithic settlements along the coast of Oman (6000–3000 cal. BC). *Journal of Archaeological Science* 40:3087–104.
- Bieler R, Kappner I, Mikkelsen PM. 2004. *Periglypta listeri* (J. E. Gray, 1838) (Bivalvia: Veneridae) in the western Atlantic: taxonomy, anatomy, life habits and distribution. *Malacologia* 46(2): 427–58.
- Culleton BJ, Kennett DJ, Ingram BL, Erlandson JM, Southon JR. 2006. Intrashell radiocarbon variability in marine mollusks. *Radiocarbon* 48(3): 387–400.
- Debenay JP, Tack DL, Ba M, Sy I. 1994. Environmental conditions, growth and production of *Anadara senilis* (Linnaeus, 1758) in a Senegal Lagoon. *Journal of Molluscan Studies* 60(2):113–21.
- Dutta K. 2008. Marine  $^{14}\text{C}$  reservoir age and Suess effect in the Indian Ocean. *Journal of Earth Science India* 1(III):175–88.
- Evans JW. 1972. Tidal growth increments in the cockle *Clinocardium nuttallii*. *Science* 176 (4033):416–7.
- Füllenbach CS, Schöne BR, Mertz-Kraus R. 2015. Strontium/lithium ratio in aragonitic shells of *Cerastoderma edule* (Bivalvia) — a new potential temperature proxy for brackish environments. *Chemical Geology* 417:341–55.
- Grossman EL, Ku T-L. 1986. Oxygen and carbon isotope fractionation in biogenic aragonite: temperature effects. *Chemical Geology: Isotope Geoscience* 59:59–74.
- Hallmann N, Burchell M, Schöne BR, Irvine GV, Maxwell D. 2009. High-resolution sclerochronological analysis of the bivalve mollusk *Saxidomus gigantea* from Alaska and British Columbia: techniques for revealing environmental archives and archaeological seasonality. *Journal of Archaeological Science* 36 (10):2353–64.
- House MR, Farrow GE. 1968. Daily growth banding in the shell of the cockle, *Cardium edule*. *Nature* 219(5161):1384–6.
- Jones DS, Arthur MA, Allard DJ. 1989. Sclerochronological records of temperature and growth from shells of *Mercenaria mercenaria* from Narragansett Bay, Rhode Island. *Marine Biology* 102:225–34.
- Khim B-K, Krantz DE, Cooper LW, Grebmeier JM. 2003. Seasonal discharge of estuarine freshwater to the western Chukchi Sea shelf identified in stable isotope profiles of mollusk shells. *Journal of Geophysical Research: Oceans* 108(C9): 3300.
- Kromer B, Lindauer S, Synal H-A, Wacker L. 2013. MAMS - a new AMS facility at the Curt-Engelhorn-Centre for Archaeometry, Mannheim, Germany. *Nuclear Instruments and Methods in Physics Research B* 294:11–3.
- Lindauer S, Kromer B. 2013. Carbonate sample preparation for  $^{14}\text{C}$  dating using an elemental analyzer. *Radiocarbon* 55(2–3):364–72.
- Marali S, Schöne BR. 2015. Oceanographic control on shell growth of *Arctica islandica* (Bivalvia) in surface waters of Northeast Iceland — implications for paleoclimate reconstructions. *Palaeogeography, Palaeoclimatology, Palaeoecology* 420:138–49.

- Milano S, Schöne BR, Witbaard R. 2015. Changes of shell microstructural characteristics of *Cerastoderma edule* (Bivalvia) — a novel proxy for water temperature. *Palaeogeography, Palaeoclimatology, Palaeoecology*. doi:10.1016/j.palaeo.2015.09.051.
- Ohno T. 1989. Palaeotidal characteristics determined by micro-growth patterns in bivalves. *Palaeontology* 32(2):217–63.
- Pape E, Muthumbi A, Kamanu CP, Vanreusel A. 2008. Size-dependent distribution and feeding habits of *Terebralia palustris* in mangrove habitats of Gazi Bay, Kenya. *Estuarine, Coastal and Shelf Science* 76(4):797–808.
- Patel B, Patel S, Balani MC, Pawar S. 1978. Flux of certain radionuclides in the blood-clam *Anadara granosa* Linnaeus under environmental conditions. *Journal of Experimental Marine Biology and Ecology* 35(2):177–95.
- Petchey F, Clark G. 2011. Tongatapu hardwater: investigation into the  $^{14}\text{C}$  marine reservoir offset in lagoon, reef and open ocean environments of a limestone island. *Quaternary Geochronology* 6(6): 539–49.
- Petchey F, Ulm S, David B, McNiven I, Asmussen B, Tomkins H, Dolby N, Aplin K, Richards T, Rowe C, Leavesley M, Mandui H. 2013. High-resolution radiocarbon dating of marine materials in archaeological contexts: radiocarbon marine reservoir variability between *Anadara*, *Gafrarium*, *Batissa*, *Polymesoda* spp. and Echinoidea at Caution Bay, Southern Coastal Papua New Guinea. *Archaeological and Anthropological Sciences* 5(1):69–80.
- Phillips CS, Mosseri-Marlio CE. 2002. Sustaining change: the emerging picture of the Neolithic to Iron Age subsistence economy at Kalba, Sharjah Emirate, UAE. *Fifth International Symposium on the Archaeozoology of Southwestern Asia and Adjacent areas, Amman, Jordan*. Groningen: ARC-Publicities.
- Rodelli MR, Gearing JN, Gearing PJ, Marshall N, Sasekumar A. 1984. Stable isotope ratio as a tracer of mangrove carbon in Malaysian ecosystems. *Oecologia* 61(3):326–33.
- Rollins HB, Sandweiss DH, Rollins JC. 1990. Mollusks and coastal archaeology; a review. In: *Decade of North American Geology, Centennial Special Volume 4 Archaeological Geology of North America*. Denver: Geological Society of America. p 467–78.
- Schöne BR. 2008. The curse of physiology – challenges and opportunities in the interpretation of geochemical data from mollusk shells. *Geo-Marine Letters* 28(5):269–85.
- Schöne BR, Surge DM. 2012. *Bivalve Sclerochronology and Geochemistry. Part N (Revised), Volume 1 Mollusca 6 Bivalvia*. Lawrence: Paleontological Institute University of Kansas. p 1–24.
- Schöne BR, Dunca E, Fiebig J, Pfeiffer M. 2005a. Mutvei's solution: an ideal agent for resolving microgrowth structures of biogenic carbonates. *Palaeogeography, Palaeoclimatology, Palaeoecology* 228(1–2):149–66.
- Schöne BR, Fiebig J, Pfeiffer M, Gleß R, Hickson J, Johnson ALA, Dreyer W, Oschmann W. 2005b. Climate records from a bivalved Methuselah (*Arctica islandica*, Mollusca; Iceland). *Palaeogeography, Palaeoclimatology, Palaeoecology* 228(1–2):130–48.
- Schöne BR, Wanamaker AD Jr, Fiebig J, Thébault J, Kreutz K. 2011. Annually resolved  $\delta^{13}\text{C}$  shell chronologies of long-lived bivalve mollusks (*Arctica islandica*) reveal oceanic carbon dynamics in the temperate North Atlantic during recent centuries. *Palaeogeography, Palaeoclimatology, Palaeoecology* 302(1–2):31–42.
- Soulet G. 2015. Methods and codes for reservoir–atmosphere  $^{14}\text{C}$  age offset calculations. *Quaternary Geochronology* 29:97–103.
- Southon J, Kashgarian M, Fontugne M, Metivier B, Yim WW-S. 2002. Marine reservoir corrections for the Indian Ocean and Southeast Asia. *Radiocarbon* 44(1):167–80.
- Tebano T, Paulay G. 2000. Variable recruitment and changing environments create a fluctuating resource: the biology of *Andara uropigimelana* (Bivalvia: Arcidae) on Tarawa Atoll. *Atoll Research Bulletin* 488:1–15.
- von Bertalanffy L. 1938. A quantitative theory of organic growth (inquiries on growth laws. II). *Human Biology* 10:181–213.
- Wacker L, Fülöp RH, Hajdas I, Molnár M, Rethemeyer J. 2013. A novel approach to process carbonate samples for radiocarbon measurements with helium carrier gas. *Nuclear Instruments and Methods in Physics Research B* 294:214–7.
- Wanamaker AD Jr, Kreutz KJ, Schöne BR, Introne DS. 2011. Gulf of Maine shells reveal changes in seawater temperature seasonality during the Medieval Climate Anomaly and the Little Ice Age. *Palaeogeography, Palaeoclimatology, Palaeoecology* 302(1–2):43–51.
- Zazzo A. 2014. Bone and enamel carbonate diagenesis: a radiocarbon prospective. *Palaeogeography, Palaeoclimatology, Palaeoecology* 416:168–78.
- Zazzo A, Munoz O, Saliège J-F, Moreau C. 2012. Variability in the marine radiocarbon reservoir effect in Muscat (Sultanate of Oman) during the 4th millennium BC: reflection of taphonomy or environment? *Journal of Archaeological Science* 39(7):2559–67.
- Zazzo A, Lebon M, Chiotti L, Comby C, Delqué-Kolic E, Nespoulet R, Reiche I. 2013. Can we use calcined bones for radiocarbon dating the Paleolithic? *Radiocarbon* 55(2–3):1409–21.
- Zazzo A, Munoz O, Badel E, Béguier I, Genchi F, Marcucci LG. 2016. A revised radiocarbon chronology of the aceramic shell midden of Ra's Al-Hamra 6 (Muscat, Sultanate of Oman): implication for occupational sequence, marine reservoir age, and human mobility. *Radiocarbon* 58(2):383–95.